Mechanical and thermo-mechanical properties of carbon nanotube reinforced composites

Chensong Dong[a]

[a] Department of Mechanical Engineering, Curtin University, GPO Box 1987, Perth, WA 6845, Australia
Published online: 01 Apr 2014.

PLEASE SCROLL DOWN FOR ARTICLE

Taylor & Francis
Taylor & Francis Group

Mechanical and thermo-mechanical properties of carbon nanotube reinforced composites

Chensong Dong*

Department of Mechanical Engineering, Curtin University, GPO Box 1987, Perth, WA 6845, Australia

A study on the mechanical and thermo-mechanical properties of carbon nanotube (CNT) reinforced nanocomposites is presented in this article. Mori–Tanaka method is used for modeling the effective stiffness and coefficient of thermal expansion. Regression formulas were developed to describe the effects of CNT orientation, aspect ratio, and CNT volume fraction. Given the statistical distributions of CNT orientations and aspect ratios, the effective properties can be conveniently derived by numerical integration using these formulas.

Keywords: carbon nanotube (CNT); stiffness; coefficient of thermal expansion (CTE)

Nomenclature

a	Aspect ratio
A	Concentration factor relating to the average strain in the effective reinforcement to that of the unknown effective material in which it is embedded
C	Stiffness tensor of composites in the local coordinate system
$\overline{\textbf{C}}$	Stiffness tensor of composites in the global coordinate system
C_{2D}	Stiffness of 2D random composites
C_{3D}	Stiffness of 3D random composites
C_f	Stiffness tensor of fibers
C_m	Stiffness tensor of matrix
$l_1, l_2, l_3, m_1, m_2, m_3, n_1, n_2, n_3$	Directional cosines
S	Eshelby's tensor
T	Transformation matrix for stress
T_ε	Transformation matrix for strain
V_f	Fiber volume fraction
α	CTE in the local coordinate system
$\overline{\textbf{α}}$	CTE in the global coordinate systems
α_{2D}	CTE of 2D random composites
α_{3D}	CTE of 3D random composites
$α_f$	CTE of fibers
$α_m$	CTE of matrix
ε	Strain tensors in the local coordinate system

*Email: c.dong@curtin.edu.au

$\overline{\varepsilon}$	Strain tensors in the global coordinate system
Φ, θ, β	Euler angles
σ	Stress tensors in the local coordinate system
$\overline{\sigma}$	Stress tensors in the global coordinate system

1. Introduction

Since the discovery of multi-walled carbon nanotubes in 1991 by Iijima [1] and subsequent synthesis of single-walled carbon nanotubes (SWCNTs) [2,3], numerous experimental and theoretical studies have been carried out to investigate the electronic, chemical, and mechanical properties of carbon nanotubes (CNTs). SWCNT–polymer composites are theoretically predicted to have both exceptional mechanical and special functional properties that carbon fiber–polymer composites cannot offer [4].

The magnitude of the coefficient of thermal expansion (CTE) depends on the structure of the materials. For single-phase materials, CTE is determined from atomic bonding, molecular structure, and molecular assembly. An elevated temperature would increase thermal energy and lead to increasing atomic movement. Weak atomic bonding with a low bonding energy would show a large CTE owing to an increasing interatomic distance. For multi-phase materials, such as composites, the CTE is dependent on each component phase and also the interactions between each phase. Weak interface bonding between phases could not effectively incorporate the contributions of each component while strong interface bonding could compromise each ingredient for thermal-expansion properties.

Molecular dynamics (MD) predictions [5] have shown that the axial CTEs of CNTs are negative in a wide low-temperature range, and vary nonlinearly with the temperature. These axial CTEs may become positive as the temperature increases. This indicates that the CTE could be significantly reduced by adding CNTs into a polymer matrix, provided good interfacial bonding is achieved.

Wei *et al.* [6] investigated the CTE of SWCNT–polyethylene composites through MD simulation shows that the CTE increases with nanotube loading, which is attributed to phonon modes and Brownian motions. Guo *et al.* [7] studied the properties of polyacrylonitrile/SWCNT composite films and the CTE of composite was 1.7×10^{-6} °C^{-1} at a weight loading of 40%. Xu *et al.* [8] found that the CTE of SWCNT/poly(vinylidene fluoride) composites decreased with increased SWCNT content. Wang *et al.* [9] studied the CTEs of nanocomposites reinforced by functionalized CNTs, and found that a reduction of 52% is observed below the glass transition temperature (T_g). However, the CTE above T_g increases significantly due to the contribution of phonon modes and Brownian motions. These studies show inconsistent results, which can be attributed to two competing mechanisms: (1) the high stiffness and low CTE will restrain the expansion of the matrix, causing the decrease in the CTE; (2) the phonon modes and Brownian motions increase the CTE. The resulting CTE is a combined effect of these two mechanisms, and highly dependent on the interfacial bonding.

Extensive investigations into the preparation and characterization of SWCNT–polymer composites have been reported [10,11]. However, the properties of the composites are not as expected because of poor dispersion and weak interfacial bonding. One possible solution to acquire high-performance nanocomposites is functionalization. Some recent experimental results indicate that the mechanical properties of SWCNT–polymer composites are significantly enhanced through functionalization [9,12,13], which demonstrates potential applications in structural and multifunctional materials.

Halpin–Tsai equation [10,14], Mori–Tanaka method [15–17], and finite element analysis [18] have been used for predicting the properties of composites. In this study, the stiffness and CTE of CNT reinforced polymer nanocomposites in various configurations, i.e., unidirectional, 2D random, and 3D random, are studied. The effects of CNT orientation, aspect ratio, and CNT volume content are investigated using Mori–Tanaka method. The distribution of CNT is characterized statistically and the corresponding stiffness and CTE are predicted. The results provide a practical insight into the reinforcing effects of CNT for polymers.

2. Approach

2.1. Mori-Tanaka method

The elastic and thermo-elastic properties of CNT composites are modeled using the method proposed by Taya et al. [19,20] based on Eshelby's inclusion theory [21] and Mori–Tanaka's mean field theory [15]. It is proved by Seidel and Lagoudas [16] that the Mori–Tanaka method provides accurate results. Using the Mori–Tanaka method, the effective stiffness is given by

$$\mathbf{C} = [(1 - V_\mathrm{f})\mathbf{C_m} + V_\mathrm{f}\mathbf{C_f A}][(1 - V_\mathrm{f})\mathbf{I} + V_\mathrm{f}\mathbf{A}]^{-1} \tag{1}$$

$$\mathbf{A} = \left[\mathbf{I} + \mathbf{S C_m^{-1}}(\mathbf{C_f} - \mathbf{C_m})\right]^{-1} \tag{2}$$

For a general ellipsoidal inclusion, the components of Eshelby's tensor S_{ijkl} are dependent on the aspect ratio, and their expressions can be found in the literature [18]. For a fiber-like inclusion, e.g., CNT ($x_1 = x_2 < x_3$), the aspect ratio is given by $a = x_3/x_1 = l/d$, as shown in Figure 1.

In the stiffness tensor, the longitudinal and transverse stiffness components are C_{33} and C_{11}, respectively. For the purpose of comparison, the normalized longitudinal and transverse stiffness components are defined as

$$C_\mathrm{L}^* = C_{33}/C_\mathrm{m} \tag{3}$$

$$C_\mathrm{T}^* = C_{11}/C_\mathrm{m} \tag{4}$$

The effective CTE of the composite is given by

$$\boldsymbol{\alpha} = \boldsymbol{\alpha_m} + V_\mathrm{f}\left\{\mathbf{C_m} + (\mathbf{C_f} - \mathbf{C_m})\left[(1 - V_\mathrm{f})\mathbf{S} + V_f\mathbf{I}\right]\right\}^{-1}\mathbf{C_f}(\boldsymbol{\alpha_f} - \boldsymbol{\alpha_m}) \tag{5}$$

The longitudinal and transverse CTEs are α_{33} and α_{11}, respectively. Similarly, the normalized longitudinal and transverse CTEs are defined as

$$\alpha_\mathrm{L}^* = \alpha_{33}/\alpha_\mathrm{m} \tag{6}$$

$$\alpha_\mathrm{T}^* = \alpha_{11}/\alpha_\mathrm{m} \tag{7}$$
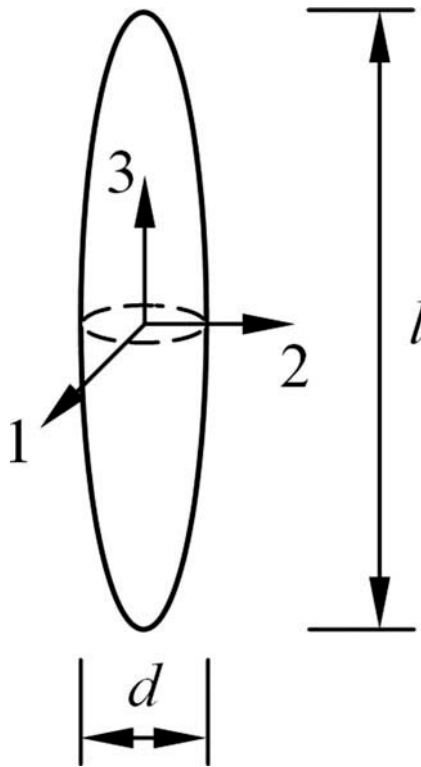
Figure 1.   A fiber-like inclusion.

2.2.   Transformation

When nanotubes are oriented at an arbitrary angle, the effective stiffness and CTE need to be transformed to the global coordinate system. This can be conveniently done using Euler angles, ϕ, θ, and β, which are referred to, respectively, as precession, nutation, and spin, as shown in Figure 2. For unidirectional composites, $\phi = \theta = \beta = 0$; for 2D random
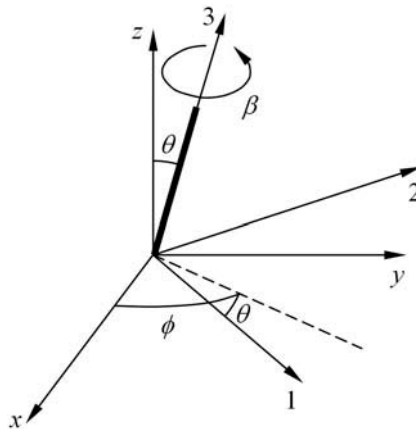
Figure 2.   Euler angles.

composites, $\phi = \beta = 0$ and $0 \le \theta \le \pi$; and for 3D random composites, $\beta = 0$, $0 \le \theta, \phi \le \pi$.

From the Euler angles, the directional cosines can be obtained, i.e.

$$
\begin{array}{lll}
l_1 = \cos\phi\cos\theta & m_1 = \sin\phi\cos\theta & n_1 = -\sin\theta \\
l_2 = -\sin\phi & m_2 = \cos\phi & n_2 = 0 \\
l_3 = \cos\phi\sin\theta & m_3 = \sin\phi\sin\theta & n_3 = \cos\theta
\end{array}
\tag{8}
$$

The transformation matrix is given by

$$
\mathbf{T} =
\begin{bmatrix}
l_1^2 & m_1^2 & n_1^2 & 2m_1n_1 & 2l_1n_1 & 2l_1m_1 \\
l_2^2 & m_2^2 & n_2^2 & 2m_2n_2 & 2l_2n_2 & 2l_2m_2 \\
l_3^2 & m_3^2 & n_3^2 & 2m_3n_3 & 2l_3n_3 & 2l_3m_3 \\
l_2l_3 & m_2m_3 & n_2n_3 & m_2n_3+m_3n_2 & l_2n_3+l_3n_2 & l_2m_3+l_3m_2 \\
l_1l_3 & m_1m_3 & n_1n_3 & m_1n_3+m_3n_1 & l_1n_3+l_3n_1 & l_1m_3+l_3m_1 \\
l_1l_2 & m_1m_2 & n_1n_2 & m_1n_2+m_2n_1 & l_1n_2+l_2n_1 & l_1m_2+l_2m_1
\end{bmatrix}
\tag{9}
$$

The transformation of stress tensors is given with respect to Figure 3 by

$$
\boldsymbol{\sigma} = \mathbf{T}\overline{\boldsymbol{\sigma}}
\tag{10}
$$

where $\overline{\boldsymbol{\sigma}}$ and $\boldsymbol{\sigma}$ are the stress tensors in the global (oxy) and local $(ox'y')$ coordinate systems, respectively.

The transformation of strain vectors is given by

$$
\boldsymbol{\varepsilon} = \mathbf{T^T}\overline{\boldsymbol{\varepsilon}}
\tag{11}
$$

where $\overline{\boldsymbol{\varepsilon}}$ and $\boldsymbol{\varepsilon}$ are the strain tensors in the global (oxy) and local $(ox'y')$ coordinate systems, respectively.

Therefore, the stiffness tensor in the global coordinate system is given by

$$
\overline{\mathbf{C}} = \mathbf{T^{-1}}\mathbf{C}\left(\mathbf{T^{-1}}\right)^{\mathbf{T}}
\tag{12}
$$

The normalized effective stiffness as a function of orientation angle is defined as
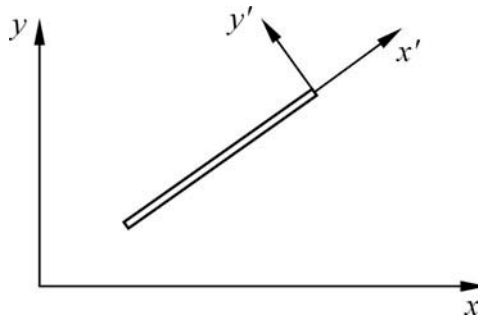

Figure 3. Transformation between coordinate systems.

$$\bar{C}^*(\theta) = \bar{C}_{33}/C_{\mathrm{m}} \tag{13}$$

The CTE in the global coordinate system is given by

$$\bar{\boldsymbol{\alpha}} = \mathbf{T}^{\mathbf{T}}\boldsymbol{\alpha} \tag{14}$$

where $\bar{\boldsymbol{\alpha}}$ and $\boldsymbol{\alpha}$ are the CTE in the global (oxy) and local ($ox'y'$) coordinate systems, respectively.

The normalized effective CTE as a function of orientation angle is defined as

$$\bar{\alpha}^*(\theta) = \bar{\alpha}_{33}/\alpha_{\mathrm{m}} \tag{15}$$

In addition to stiffness and CTE, Eshelby's tensors also need to be transformed in such a way that

$$\bar{\mathbf{S}} = \mathbf{T}^{\mathbf{T}}\mathbf{S}\mathbf{T} \tag{16}$$

where $\bar{\mathbf{S}}$ is the transformed Eshelby's tensor.

2.3.   *Effects of parameters*

The effects of CNT orientation, CNT volume fraction on the effective properties of unidirectional, 2D random, and 3D random composites were studied. Based on the data from the literature, a SWCNT loading of 1% by weight corresponds to approximately 0.743% by volume.

In this study, the effective longitudinal and transverse moduli of CNT at the room temperature were taken to be 704 GPa and 346 GPa, respectively [16]. The longitudinal and transverse CTEs of SWCNTs at the room temperature were estimated to be -12×10^{-6} °C^{-1} and $-1.5 \pm 2 \times 10^{-6}$ °C^{-1}, respectively [22–24], which were further validated using X-ray measurements [25]. The matrix was epoxy. Its modulus and CTE are 3 GPa and 6.4×10^{-5} °C^{-1}, respectively.

There are numerous examples in the literature, which suggest that above a critical concentration of CNTs, the properties of either drop or the reinforcement efficiency decreases considerably [26,27]. Thus, in this study, only CNT loadings up to 5% (v/v) were considered.

3.   **Results**

3.1.   *Effects of orientation*

When the aspect ratio is 500 and the CNT volume fraction is 1%, the normalized effective stiffness vs. the orientation angle, θ, is shown in Figure 4. The longitudinal direction of the CNT is defined to be $\theta = 0$. From Equation (12), it can be derived that the stiffness is a function of $\cos^4\theta$. The relationship between the normalized stiffness and CNT orientation angle is given by

$$\bar{C}^*(\theta) = C_{\mathrm{T}}^* + \left(C_{\mathrm{L}}^* - C_{\mathrm{T}}^*\right)\cos^4\theta \tag{17}$$

Likewise, the normalized effective CTE vs. the orientation angle is shown in Figure 5. Similarly, the longitudinal direction of the CNT is defined to be $\theta = 0$. From Equation (14),
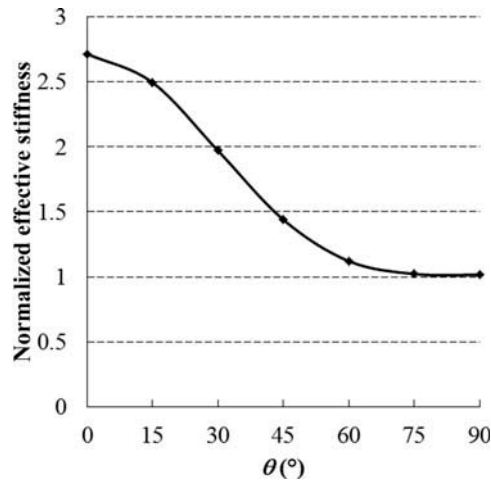
Figure 4. Normalized effective stiffness vs. CNT orientation for aspect ratio 500 and CNT volume fraction 1%.
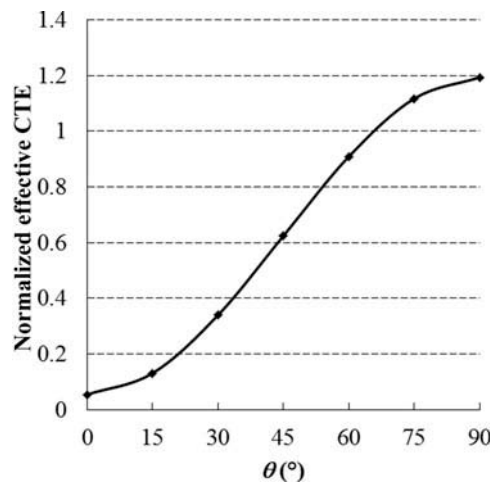
Figure 5. Normalized effective CTE vs. CNT orientation for aspect ratio 500 and CNT volume fraction 1%.

it can be derived that the effective CTE is a function of $\sin^2\theta$. The relationship between the normalized CTE and CNT orientation angle is given by

$$\bar{\alpha}^*(\theta) = \alpha_L^* + \left(\alpha_T^* - \alpha_L^*\right)\sin^2\theta \qquad (18)$$

3.2. Orientation average

The effective modulus of a 2D random composite is given by taking the orientation average, i.e.

$$C_{2D}^* = \frac{\int_0^{\frac{\pi}{2}} \bar{C}^*(\theta)\, d\theta}{\int_0^{\frac{\pi}{2}} d\theta} = \frac{2}{\pi} \int_0^{\frac{\pi}{2}} \bar{C}^*(\theta)\, d\theta \tag{19}$$

Substituting Equation (17) into Equation (19) yields

$$C_{2D}^* = \frac{3}{8} C_L^* + \frac{5}{8} C_T^* \tag{20}$$

The effective CTE of a 2D random composite is given by

$$\alpha_{2D}^* = \frac{\int_0^{\frac{\pi}{2}} \bar{C}^*(\theta)\bar{\alpha}^*(\theta)\, d\theta}{\int_0^{\frac{\pi}{2}} \bar{C}^*(\theta)\, d\theta} \tag{21}$$

Substituting Equations (17) and (18) into Equation (21) yields

$$\alpha_{2D}^* = \frac{\left(5C_L^* + 3C_T^*\right)\alpha_L^* + \left(C_L^* + 7C_T^*\right)\alpha_T^*}{2(3C_L^* + 5C_T^*)} \tag{22}$$

Likewise, the effective stiffness of a 3D random composite is given by

$$C_{3D}^* = \frac{\int_0^{\frac{\pi}{2}} \bar{C}^*(\theta) \sin\theta\, d\theta}{\int_0^{\frac{\pi}{2}} \sin\theta\, d\theta} = \int_0^{\frac{\pi}{2}} \bar{C}^*(\theta) \sin\theta\, d\theta \tag{23}$$

Substituting Equation (17) into Equation (23) yields

$$C_{3D}^* = \frac{1}{5} C_L^* + \frac{4}{5} C_T^* \tag{24}$$

Likewise, the effective CTE of a 3D random composite is given by

$$\alpha_{3D}^* = \frac{\int_0^{\frac{\pi}{2}} \bar{C}^*(\theta)\bar{\alpha}^*(\theta) \sin\theta\, d\theta}{\int_0^{\frac{\pi}{2}} \bar{C}^*(\theta) \sin\theta\, d\theta} \tag{25}$$

Substituting Equations (17) and (18) into Equation (25) yields

$$\alpha_{3D}^* = \frac{\left(15C_L^* + 20C_T^*\right)\alpha_L^* + \left(6C_L^* + 64C_T^*\right)\alpha_T^*}{21(C_L^* + 4C_T^*)} \tag{26}$$

3.3. Aspect ratio

The effective longitudinal and transverse stiffness vs. the aspect ratio for the CNT reinforced composites at various CNT volume fractions from 1% to 5% is plotted in Figure 6. It is shown that the longitudinal stiffness increases with the aspect ratio while little change is seen for the transverse stiffness. When the aspect ratio is greater than 100, the change in stiffness becomes less.
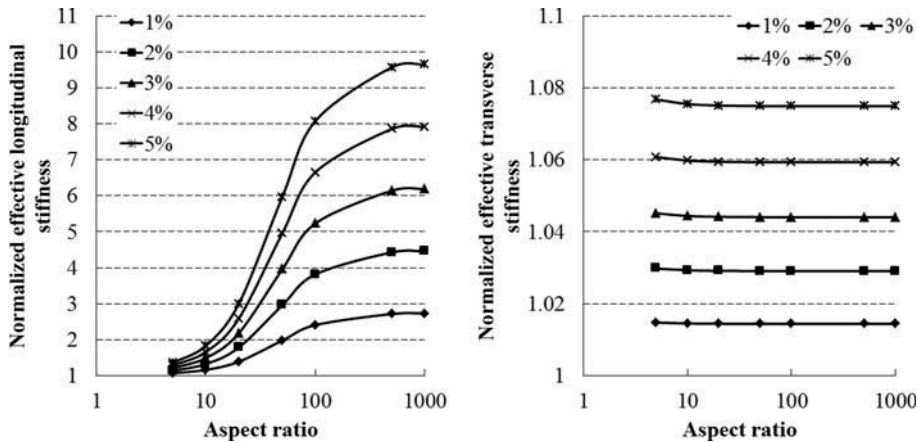
Figure 6.   Normalized effective stiffness vs. aspect ratio.
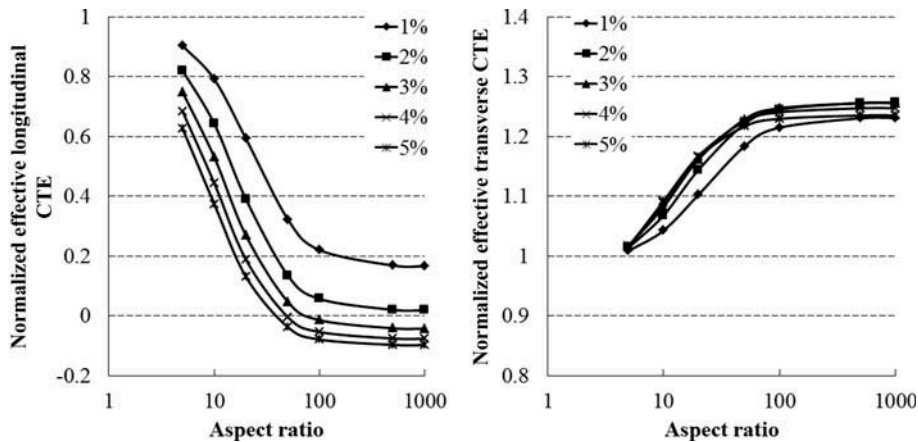
Figure 7.   Normalized effective CTE vs. aspect ratio.

The normalized effective longitudinal and transverse CTEs vs. the aspect ratio for the CNT reinforced composites at various CNT volume fractions from 1% to 5% is plotted in Figure 7. It is shown that the longitudinal CTE decreases with the increasing aspect ratio while the transverse CTE increases with the decreasing aspect ratio. When the aspect ratio is greater than 100, the change in CTE becomes less.

3.4.   *CNT volume fraction*

The normalized effective stiffness of the CNT composites vs. the CNT volume fraction is shown in Figure 8 for two aspect ratios, $a = 10$ and $a = 1000$, respectively. For both aspect ratios, when the CNT volume fraction is low (up to 5%), both the longitudinal stiffness and transverse stiffness of the CNT composites approximately linearly increases with the CNT volume fraction. The effective stiffness can be expressed by the following regression formulas.
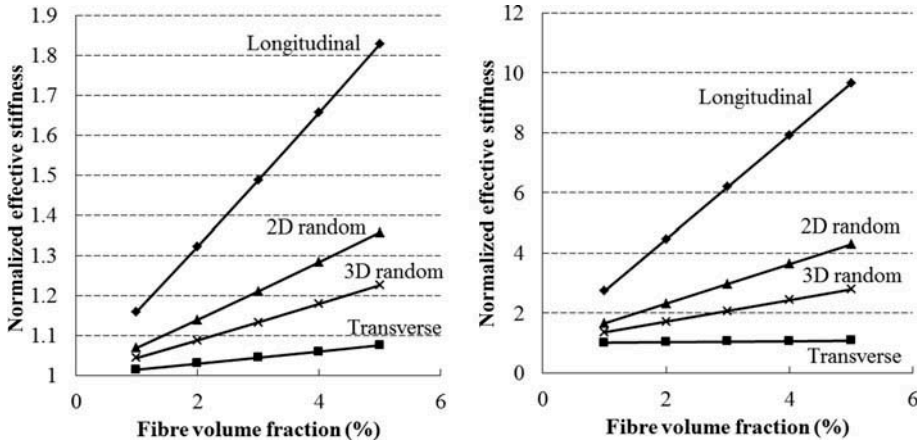
Figure 8.   Normalized effective stiffness vs. CNT volume fraction for $a = 10$ (left) and $a = 1000$ (right).
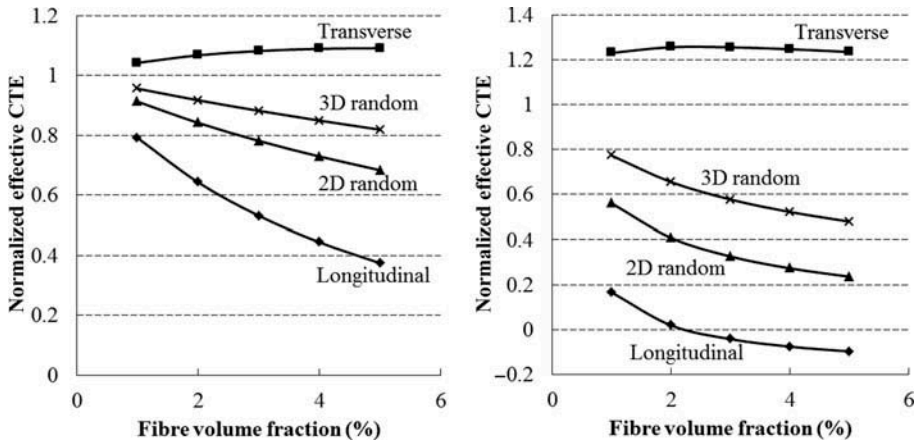
Figure 9.   Normalized effective CTE vs. CNT volume fraction for $a = 10$ (left) and $a = 1000$ (right).

Likewise, the normalized effective CTE of the CNT composites vs. the CNT volume fraction is shown in Figure 9 for two aspect ratios, $a = 10$ and $a = 1000$, respectively. For both aspect ratios, the longitudinal CTE decreases with the increasing CNT volume fraction while the transverse CTE shows little change with the CNT volume fraction.

3.5.   Regression formulas

It is shown in Figure 6 that the longitudinal stiffness vs. the aspect ratio shows a dose–response relationship, i.e.

$$C_L^*(a) = c_1 + \frac{c_2 - c_1}{1 + \left(\frac{x_0}{a}\right)^p} \tag{27}$$

where c_1, c_2, x_0, and p are constants. It is shown from the data, as shown in Figure 6, that c_1 and c_2 are functions of V_f. The final regression formula for the longitudinal stiffness is then given by

$$C_L^*(V_f, a) = 1 + 0.03V_f + \frac{1.71V_f}{1 + \left(\dfrac{43.65}{a}\right)^{1.7}} \tag{28}$$

The effective transverse stiffness is only dependent on the CNT volume fraction, and the corresponding regression formula is

$$C_T^*(V_f) = 1 + 0.015V_f \tag{29}$$

In a similar way, the longitudinal and transverse CTEs can also be expressed by dose–response formulas, which are given by

$$\alpha_L^*(V_f, a) = -0.066 + 0.35V_f^{-0.66} + \frac{1.066 - 0.023V_f - 0.35V_f^{-0.66}}{1 + \left(\dfrac{a}{-6.52 + 28.03V_f^{-0.34}}\right)^{1.65}} \tag{30}$$

$$\alpha_T^*(V_f, a) = 1 + \frac{0.2}{1 + \left(\dfrac{14.29 + 9.81V_f^{-2.5}}{a}\right)^{1.65}} \tag{31}$$

4. Effects of statistical distributions

When there are CNTs of various aspect ratios in the range between a_1 and a_2, the normalized effective stiffness is derived by taking the aspect ratio average, which is given by

$$C_L^* = \int_{a_1}^{a_2} C_L^*(a)f(a)\,\mathrm{d}a \tag{32}$$

Likewise, the normalized effective CTE is given by

$$\alpha_L^* = \frac{\int_{a_1}^{a_2} \alpha_L^*(a)C_L^*(a)f(a)\,\mathrm{d}a}{\int_{a_1}^{a_2} C_L^*(a)f(a)\,\mathrm{d}a} \tag{33}$$

When the aspect ratios are uniformly distributed, the normalized effective longitudinal stiffness is derived by substituting Equation (28) into Equation (34), which is given by

$$C_L^* = 1 + 0.03V_f + \frac{1.71V_f}{a_2 - a_1}\left\{ a_2\left[{}_2F_1\left(1, -0.59; 0.41; -\left(\tfrac{43.65}{a_2}\right)^{1.7}\right)\right] - a_1\left[{}_2F_1\left(1, -0.59; 0.41; -\left(\tfrac{43.65}{a_1}\right)^{1.7}\right)\right] \right\} \tag{34}$$

where $_2F_1(\underline{a}_1, \underline{a}_2; \underline{b}_1; z) = \sum_{n=0}^{\infty} \frac{a_1^{(n)} a_2^{(n)}}{b_1^{(n)}} \frac{z^n}{n!}$ is the generalized hypergeometric function, and $x^{(n)} = x(x+1)(x+2)\cdots(x+n-1), \quad n \geq 1$ is the rising factorial or Pochhammer symbol.

For any other distributions, the normalized effective longitudinal stiffness can be derived via numerical integration.

For the normalized effective longitudinal and transverse CTEs, a closed form solution cannot be found, and numerical integration is needed. The effective CTE of 2D and 3D random composites can be obtained by substituting the longitudinal and transverse CTEs into Equations (22) and (26), respectively.

4.1. Uniform distributions

The stiffness and CTE for a number of uniform distributions of aspect ratios are shown in Table 1. It is shown that when the aspect ratio is greater than 100, both the stiffness and CTE are approximately constant.

4.2. Normal distributions

The stiffness and CTE for a number of normal distributions of aspect ratios are shown in Table 2. It is shown that if the aspect ratios are assumed to be normally distributed, the stiffness and CTE are mainly dependent on the mean.

4.3. Weibull distributions

The stiffness and CTE for a number of Weibull distributions of aspect ratios are shown in Table 3. It is shown that the stiffness and CTE are mainly dependent on the scale

Table 1.   Stiffness and CTE for uniform distributions.

Range	C_L^*	α_L^*	α_T^*
5–50	1.5504	0.5750	1.1009
5–100	1.9102	0.4463	1.1383
50–100	2.6165	0.3661	1.1717
5–1000	2.2340	0.3045	1.1883
100–500	2.6484	0.2970	1.1954
100–1000	2.6911	0.2910	1.1975
500–1000	2.7253	0.2861	1.1993

Table 2.   Stiffness and CTE for normal distributions.

Mean	Standard deviation	C_L^*	α_L^*	α_T^*
500	200	2.7003	0.2896	1.1980
500	100	2.7113	0.2881	1.1986
500	50	2.7129	0.2879	1.1986
150	50	2.5186	0.3163	1.1886
400	50	2.7003	0.2897	1.1980
600	50	2.7201	0.2869	1.1990
750	50	2.7264	0.2860	1.1993

Table 3. Stiffness and CTE for Weibull distributions.

Shape parameter	Scale parameter	C_L^*	α_L^*	α_T^*
1.5	500	2.6391	0.2987	1.1934
2	500	2.6708	0.2938	1.1964
2.5	500	2.6829	0.2920	1.1971
3	500	2.6914	0.2909	1.1976
1.5	200	2.5107	0.3194	1.1825
1.5	300	2.5791	0.3080	1.1887
1.5	400	2.6171	0.3020	1.1917
3	200	2.5873	0.3059	1.1924
3	300	2.6101	0.3025	1.1935
3	400	2.6679	0.2942	1.1964

parameter. When the scale parameter increases, the longitudinal stiffness increases but the longitudinal CTE decreases.

If the aspect ratio a and orientation angle θ are independent of each other, the effective stiffness of 2D and 3D random composites can be obtained by substituting Equations (29) and (36) into Equations (20) and (24), respectively.

5. Conclusions

The stiffness and CTE of CNT reinforced nanocomposites were studied with the aid of Mori–Tanaka method. The effects of CNT volume fraction, aspect ratio, and orientation were investigated. It is shown that the effective stiffness linearly increases with CNT volume fraction from 1% to 5%. The longitudinal CTE decreases with CNT volume fraction while the transverse CTE shows little change with CNT volume fraction. The longitudinal stiffness increases with the aspect ratio while little change is seen for the transverse stiffness. When the aspect ratio is greater than 100, the change in stiffness becomes less. The longitudinal CTE decreases with the increasing aspect ratio while the transverse CTE increases with the aspect ratio. When the aspect ratio is greater than 100, the change in CTE becomes less.

Regression formulas were developed to relate the stiffness and CTE to CNT volume fraction, aspect ratio, and orientation. Using these formulas, if the distribution of CNT is known, the stiffness and CTE can be conveniently obtained by numerical integration. A number of uniform, normal, and Weibull distributions were studied.

References

[1] S. Iijima, *Helical microtubules of graphitic carbon*, Nature 354 (1991), pp. 56–58. doi:10.1038/354056a0
[2] S. Iijima and T. Ichihashi, *Single-shell carbon nanotubes of 1-nm diameter*, Nature 363 (1993), pp. 603–605. doi:10.1038/363603a0
[3] D.S. Bethune, C.H. Klang, M.S. de Vries, G. Gorman, R. Savoy, J. Vazquez, and R. Beyers, *Cobalt-catalysed growth of carbon nanotubes with single-atomic-layer walls*, Nature 363 (1993), pp. 605–607. doi:10.1038/363605a0
[4] E.T. Thostenson and T.-W. Chou, *On the elastic properties of carbon nanotube-based composites: Modelling and characterization*, J. Phys. D: Appl. Phys. 36 (5) (2003), p. 573–582. doi:10.1088/0022-3727/36/5/323

[5] A. Alamusi, N. Hu, B. Jia, M. Arai, C. Yan, J. Li, Y. Liu, S. Atobe, and H. Fukunaga, *Prediction of thermal expansion properties of carbon nanotubes using molecular dynamics simulations*, Comput. Mater. Sci. 54 (2012), pp. 249–254. doi:10.1016/j.commatsci.2011.10.015

[6] C. Wei, D. Srivastava, and K. Cho, *Thermal expansion and diffusion coefficients of carbon nanotube–polymer composites*, Nano Lett. 2 (6) (2002), pp. 647–650. doi:10.1021/nl025554+

[7] H. Guo, T.V. Sreekumar, T. Liu, M. Minus, and S. Kumar, *Structure and properties of polyacrylonitrile/single wall carbon nanotube composite films*, Polymer 46 (9) (2005), pp. 3001–3005. doi:10.1016/j.polymer.2005.02.013

[8] Y. Xu, G. Ray, and B. Abdel-Magid, *Thermal behavior of single-walled carbon nanotube polymer–matrix composites*, Comp. Part A Appl. Sci. Manufact. 37 (1) (2006), pp. 114–121. doi:10.1016/j.compositesa.2005.04.009

[9] S. Wang, Z. Liang, P. Gonnet, Y. Liao, B. Wang, and C. Zhang, *Effect of nanotube functionalization on the coefficient of thermal expansion of nanocomposites*, Adv Funct. Mater. 17 (1) (2007), pp. 87–92. doi:10.1002/adfm.200600760

[10] M.T. Byrne and Y.K. Gun'ko, *Recent advances in research on carbon nanotube–polymer composites*, Adv. Mater. 22 (15) (2010), pp. 1672–1688. doi:10.1002/adma.200901545

[11] N.G. Sahoo, S. Rana, J.W. Cho, L. Li, and S.H. Chan, *Polymer nanocomposites based on functionalized carbon nanotubes*, Prog. Polym. Sci. 35 (7) (2010), pp. 837–867. doi:10.1016/j.progpolymsci.2010.03.002

[12] S. Wang, Z. Liang, T. Liu, B. Wang, and C. Zhang, *Effective amino-functionalization of carbon nanotubes for reinforcing epoxy polymer composites*, Nanotechnology 17 (6) (2006), pp. 1551–1557. doi:10.1088/0957-4484/17/6/003

[13] J. Zhu, J. Kim, H. Peng, J.L. Margrave, V.N. Khabashesku, and E.V. Barrera, *Improving the dispersion and integration of single-walled carbon nanotubes in epoxy composites through functionalization*, Nano Lett. 3 (8) (2003), pp. 1107–1113. doi:10.1021/nl0342489

[14] J.C. Halpin and N.J. Pagano, *The laminate approximation for randomly oriented fibrous composites*, J. Comp. Mater. 3 (4) (1969), pp. 720–724.

[15] T. Mori and K. Tanaka, *Average stress in matrix and average elastic energy of materials with misfitting inclusions*, Acta Metal. 21 (5) (1973), pp. 571–574. doi:10.1016/0001-6160(73)90064-3

[16] G.D. Seidel and D.C. Lagoudas, *Micromechanical analysis of the effective elastic properties of carbon nanotube reinforced composites*, Mech. Mater. 38 (8–10) (2006), pp. 884–907.

[17] V. Anumandla and R.F. Gibson, *A comprehensive closed form micromechanics model for estimating the elastic modulus of nanotube-reinforced composites*, Comp. Part A Appl. Sci. Manufact. 37 (12) (2006), pp. 2178–2185. doi:10.1016/j.compositesa.2005.09.016

[18] G.P. Tandon and G.J. Weng, *The effect of aspect ratio of inclusions on the elastic properties of unidirectionally aligned composites*, Polym. Comp. 5 (4) (1984), pp. 327–333. doi:10.1002/pc.750050413

[19] Y. Takao and M. Taya, *Thermal expansion coefficients and thermal stresses in an aligned short fiber composite with application to a short carbon fiber/aluminum*, ASME Trans. J. Appl. Mech. 52 (1985), pp. 806–810. doi:10.1115/1.3169150

[20] M. Taya and T.W. Chou, *On two kinds of ellipsoidal inhomogeneities in an infinite elastic body: An application to a hybrid composite*, Int. J. Solids Struct. 17 (6) (1981), pp. 553–563. doi:10.1016/0020-7683(81)90018-4

[21] J.D. Eshelby, *The determination of the elastic field of an ellipsoidal inclusion, and related problems*, Proc. R. Soc A Math. Phys. Eng. Sci. 241 (1226) (1957), pp. 376–396. doi:10.1098/rspa.1957.0133

[22] H. Jiang, B. Liu, Y. Huang, and K.C. Hwang, *Thermal expansion of single wall carbon nanotubes*, J. Eng. Mater. Technol. 126 (3) (2004), pp. 265–270. doi:10.1115/1.1752925

[23] Y.-K. Kwon, S. Berber, and D. Tománek, *Thermal contraction of carbon fullerenes and nanotubes*, Phys. Rev. Lett. 92 (1) (2004), 015901. doi:10.1103/PhysRevLett.92.015901

[24] R.B. Pipes and P. Hubert, *Helical carbon nanotube arrays: Thermal expansion*, Comp. Sci. Technol. 63 (11) (2003), pp. 1571–1579. doi:10.1016/S0266-3538(03)00075-7

[25] Y. Maniwa, R. Fujiwara, H. Kira, H. Tou, H. Kataura, S. Suzuki, Y. Achiba, E. Nishibori, M. Takata, M. Sakata, A. Fujiwara, and H. Suematsu, *Thermal expansion of single-walled carbon nanotube (SWNT) bundles: X-ray diffraction studies*, Phys. Rev B. 64 (24) (2001), 241402. doi:10.1103/PhysRevB.64.241402

[26] W. Jeong and M.R. Kessler, *Effect of functionalized MWCNTs on the thermo-mechanical properties of poly(5-ethylidene-2-norbornene) composites produced by ring-opening metathesis polymerization*, Carbon 47 (10) (2009), pp. 2406–2412. doi:10.1016/j. carbon.2009.04.042

[27] S. Kanagaraj, F.R. Varanda, T.V. Zhiltsova, M.S.A. Oliveira, and J.A.O. Simoes. *Mechanical properties of high density polyethylene/carbon nanotube composites*, Comp. Sci. Technol. 67 (15–16) (2007), pp. 3071–3077.